Superbanana transport in the collisional heating of a plasma column forced across a squeeze potential

Daniel H. E. Dubin

Citation: Physics of Plasmas **24**, 112120 (2017);
View online: https://doi.org/10.1063/1.5001062
View Table of Contents: http://aip.scitation.org/toc/php/24/11
Published by the American Institute of Physics

Superbanana transport in the collisional heating of a plasma column forced across a squeeze potential

Daniel H. E. Dubin
Department of Physics, UCSD, La Jolla, California 92093, USA

(Received 21 August 2017; accepted 2 November 2017; published online 28 November 2017)

When weakly collisional plasmas have locally trapped particle populations, perturbations to the plasma equilibrium (such as waves or static field-errors) can induce phase-space discontinuities in the particle distribution function that strongly enhance entropy production, plasma loss, and wave damping via superbanana transport. This paper presents a simple version of this superbanana transport process, wherein a plasma is heated as it is slowly forced back and forth across a squeeze potential (at a frequency ω that is small compared with the particle bounce frequency). The squeeze potential traps low-energy particles on either side of the squeeze, but particles with higher energy can pass through it. Trapped and passing particles have different responses to the forcing, causing a collisionless discontinuity in the distribution function at the separatrix between the trapped and passing particles. Expressions for both the adiabatic and non-adiabatic distribution functions are presented, and the heating rate caused by collisional broadening of the separatrix discontinuity is derived. The heating rate is proportional to $\sqrt{\nu\omega}$, provided that $\nu \ll \omega$, where ν is the collision rate (i.e., the $\sqrt{\nu}$ regime of superbanana theory). *Published by AIP Publishing.*
https://doi.org/10.1063/1.5001062

I. INTRODUCTION

Natural and laboratory plasmas often have several distinct locally trapped particle populations, due to the occurrence of local magnetic and/or electrostatic wells. When subjected to perturbations such as plasma waves or field errors, such configurations can exhibit enhanced "superbanana" transport:[1–3] the locally trapped particles respond to the perturbations differently from passing particles, creating discontinuities in the collisionless particle distribution function at the separatrix (or separatrices) between trapped and passing particles; and collisional relaxation of these discontinuities causes enhanced rates of entropy production, wave damping, and transport of particles, momentum, and heat. The term "superbanana" refers to the single-particle drift orbits near the separatrix energy that are perturbed by the waves or field errors.[1]

In this paper, we consider an example of superbanana transport that elucidates the basic mechanism in a simple geometry. We consider a cylindrically symmetric nonneutral plasma column in a strong uniform axial magnetic field, confined axially by surrounding cylindrical electrodes. The magnetic field is strong enough that we need not consider radial motion of the plasma at all in what follows; only axial motions are kept in the analysis. The azimuthal rotation of the plasma is also not important in the analysis since we assume cylindrical symmetry throughout.

Locally trapped particles are created by the imposition of a cylindrically symmetric squeeze potential on one cylindrical electrode near the axial center of the column (see Fig. 1); the potential pushes particles away axially from the electrode but is not large enough to cut the plasma into two. Some particles are trapped axially on either side of the squeeze potential, while particles with more energy can pass through the squeeze region from one side to the other.

To this system, a small time-dependent potential perturbation is applied: the end electrode potentials are oscillated in time at frequency ω, pushing the plasma back and forth across the squeeze barrier. For a long thin plasma column of length L, the potential changes have the effect of changing the location of the left and right plasma ends by δL_1 and δL_2, respectively. In the case of chief interest here, we take $\delta L_1 = -\delta L_2 = \delta L$ (Fig. 1), which can be accomplished by varying the end confinement potentials 180° out of phase (one is increasing as the other decreases). The overall plasma length is unchanged in this operation, but the plasma shifts to the right and left during the end potential oscillation. As the plasma moves to the right, the plasma trapped to the left of the squeeze barrier is compressed and heated, while the plasma trapped to the right is expanded and cooled, but

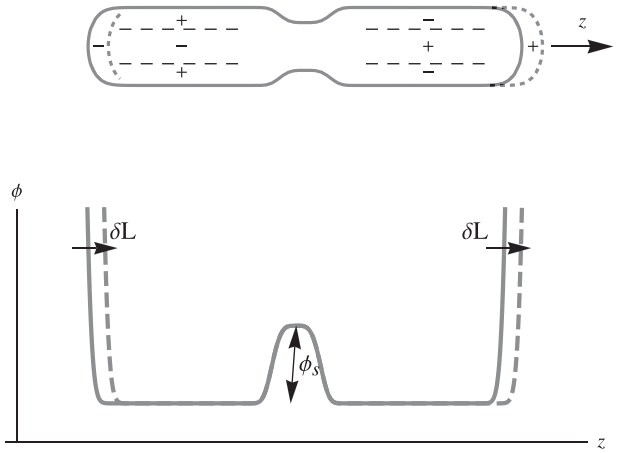

FIG. 1. Schematic of the geometry. A cylindrical plasma (top) is subjected to a central squeeze potential. The end potentials are then varied (bottom) so as to move the plasma to the right by $\delta L(t)$, across the squeeze. The density changes from this plasma motion are denoted by the plus and minus signs.

passing particles are unaffected (to first approximation). Consequently, there is a discontinuity in the collisionless plasma distribution function induced by the perturbation, located at the energy separatrix ϕ_s between trapped and passing particles.

This discontinuity can produce strong plasma heating compared with other heating mechanisms. We analyze the regime $\nu \ll \omega \ll \omega_b$, where the perturbed potential oscillates at a frequency ω much greater than the plasma collision frequency ν, but much less than the frequency ω_b at which particles bounce from end to end. In this regime, compressions and expansions can, to lowest approximation, be treated as adiabatic and one-dimensional, which allows simple and explicit expressions for the discontinuous velocity distribution function. The discontinuity at the separatrix is then collisionally broadened in energy by an amount proportional to $\sqrt{T\phi_s\nu/\omega}$, where ϕ_s is the height of the potential barrier (see Fig. 1). This narrow region of the distribution function oscillates out-of-phase with the rest of the distribution due to collisional relaxation, and consequently causes heating proportional to the region width, i.e., proportional to $\sqrt{\nu}$. (For notational convenience, all temperatures and potentials in this paper are expressed in energy units. For instance, the potential ϕ_s is related to the electrostatic potential V_s through $\phi_s = qV_s$, where q is the particle charge.)

In a bit more detail, in every period of the oscillation, trapped particles with kinetic energy K experience a reversible adiabatic change in energy $\pm 2K\delta L/L$ (where the $+$ and $-$ signs refer to the particles trapped on the left and right sides, respectively). But trapped particles with energies within $\Delta W = \sqrt{T\phi_s\nu/\omega}$ of the separatrix energy ϕ_s can collisionally cross the separatrix,[4,5] become passing, and then retrap on either side within one oscillation period, and so, the sign of the energy change becomes random for such particles as they cross and recross the separatrix. This leads to a diffusion in particle energy scaling as $\omega K^2(\delta L/L)^2$, where $K = \phi_s$ for particles at the separatrix. This irreversible process causes plasma heating. If all particles participated, the rate of temperature increase would be of order $(\omega K^2/T)(\delta L/L)^2$, where $K \sim T$ is the mean particle kinetic energy. However, these boundary-layer particles with $K \sim \phi_s$ make up only a fraction of the total particle number. For a Maxwellian distribution, this fraction is roughly $(\Delta W/\sqrt{T\phi_s})\exp(-\phi_s/T)$. So, the rate of temperature increase is $\omega(\phi_s^2/T)(\delta L/L)^2\left(\Delta W/\sqrt{T\phi_s}\right)\exp(-\phi_s/T)$, or simplifying, $\dot{T} \sim \sqrt{\nu\omega}\,(\phi_s^2/T)(\delta L/L)^2\exp(-\phi_s/T)$.

Other mechanisms can also heat the plasma when the end potentials are varied as in Fig. 1, but in the regime $\nu \ll \omega \ll \omega_b$ of interest here, the superbanana transport process dominates. For instance, wave-particle resonances can occur, causing heating which, to lowest approximation, is ν-independent (the "plateau regime"). In this regime, the heating rate is proportional to $T\omega(\omega/\omega_b)^5(\delta L/L)^2$.[6] But this mechanism has a negligible effect due to the low frequency assumed for the potential oscillation, $\omega \ll \omega_b$.

Near-adiabatic heating due to bulk viscosity can also occur. Here, the axial compression and expansion of the trapped particles causes the parallel and perpendicular temperatures to be unequal, and entropy production results as collisions relax the temperature difference. However, this mechanism causes heating of order $\nu T(\delta L/L)^2$ in the regime where $\nu \ll \omega$,[7] which scales with collisionality as the first power of ν. It is therefore approximately $\sqrt{\nu/\omega}$ smaller than superbanana heating that scales as $\sqrt{\nu}$.

Collisional drag between different species of charged particles in the plasma can also produce frictional heating proportional to ν in the regime $\omega > \nu$.[8,9] Here, the species react differently to the time-varying potential due to their different masses, and collisions dissipate the velocity differences, producing heating that scales as $\nu m(\omega\delta L)^2$. This is small compared with bulk-viscous heating when $\omega < \omega_b$. This is the Drude model for resistive dissipation, $P = I^2R$, where current I is proportional to $\omega\delta L$ and resistance R is proportional to ν.

On the other hand, if $\omega < \nu$, bulk viscous heating (or collisional drag heating) can dominate. For example, slowly oscillating plasma ends with $\omega < \nu$ will cause bulk viscosity plasma heating proportional to $T(\omega\delta L/L)^2/\nu$.[6,7] This type of heating has the expected form $P = I^2R$, where now the resistance R is proportional to $1/\nu$. Resistance R scales with collisionality in this way because as ν increases, collisions keep the system closer to thermal equilibrium, so there is less dissipation. This is similar to the damping of sound waves in molecular gases, which also scales as $1/\nu$ in the regime $\omega < \nu$,[10] due in part to molecular attenuation (bulk viscosity)[11] that manifests as a lag in the equipartition between internal energy states and translational energy.

Collisional drag heating in the regime $\omega < \nu$ has similar scaling. Here, frictional drag between species causes heating that also scales as $1/\nu$ because the species "collisionally-lock": the drag force couples the motion of each species, so they have nearly the same response to the potential oscillation.[9]

However, in the regime $\nu \ll \omega$, the intuition that follows from $P = I^2R$ fails because the collisions are so weak that near-discontinuities (boundary-layers) develop in the distribution function, and relaxation of these boundary layers dominates the heating. Consequently, scaling of the heating with ν and ω is quite different in this weak collisionality regime.

Heating proportional to $\sqrt{\nu}$, caused by a collisional boundary layer at the separatrix between trapped and passing particles, is a simple example of superbanana transport in the so-called $\sqrt{\nu}$ regime.[1–3] This regime is of importance in the neoclassical transport expected for weakly collisional fusion plasmas in devices such as stellarators or "bumpy tori."

The geometry of the heating mechanism considered here is sufficiently straightforward that expressions for plasma heating can be evaluated and compared directly with experiments. Such experimental comparisons will be considered in a separate paper.[12] Here, we lay out the theory. This geometry has been considered previously in studies of superbanana transport that involves the damping of low-frequency drift waves (trapped particle diocotron modes)[13–15] and cross-magnetic field particle transport.[4,5,16–19] In those cases, cross-magnetic field drifts and plasma rotation were

necessary ingredients in the theory. Here, these effects can be ignored, further simplifying the analysis.

Nevertheless, the self-consistent plasma response to sloshing through a squeeze potential is non-trivial even in this simple geometry. As trapped particles are compressed or expanded, the passing particles stream along the magnetic field in order to shield out the resulting potential changes. These potential changes couple the plasma response at different radii. For instance, at larger radii within the plasma, most particles are trapped by the squeeze potential, and so, a slosh to the right as shown in Fig. 1 increases the density to the left of the squeeze and decreases it to the right. However, at smaller radii, geometric effects and plasma screening reduce the squeeze potential, and here, passing particles dominate the plasma response. These particles stream to the right end of the plasma column in order to shield out the density changes caused by the trapped particles at larger radii.

In Sec. II, we consider the collisionless adiabatic response to slow variations in the external potential, including self-consistent plasma effects. In Sec. III, we determine the effect of weak collisions on the distribution function and evaluate the heating. In Sec. IV, we discuss the results and consider some outstanding questions. In Appendix A, we consider a numerical method for solution to the self-consistent problem. In Appendix B, we consider the lowest-order collisionless nonadiabatic effects on the distribution function.

II. COLLISIONLESS DISTRIBUTION FUNCTIONS UNDERGOING ADIABATIC VARIATIONS

This section describes adiabatic invariant theory for the collisionless evolution of a distribution function under slow time-variation of external potentials. For charged particles of mass m moving in a uniform magnetic field $B\hat{z}$ and a time-dependent potential $\phi(r,z,t)$, the particle energy $E = \frac{1}{2}mv^2 + \phi(r,z,t)$ is not a constant of the motion. However, there are approximately conserved (adiabatic) invariants of the motion. The perpendicular energy $E_\perp = \frac{1}{2}m(v_x^2 + v_y^2)$ is one such invariant (the "cyclotron invariant") as is the radial position r of the guiding center. Since r and $E_\perp$ are adiabatic invariants, for notational convenience, we will suppress any dependences on these variables in the following analysis, for example, writing $\phi = \phi(z,t)$.

The axial (z) motion of a particle is also constrained by the parallel adiabatic invariant J, which is the area enclosed by the orbit in the phase space of the axial motion, holding t fixed in the potential

$$J(E_z,t) = \oint p_z dz = 2\int_{z_1}^{z_2} \sqrt{2m[E_z - \phi(z,t)]}dz, \tag{1}$$

where the axial energy $E_z \equiv E - E_\perp$, and z_1 and z_2 are turning-points of the axial motion, found from the roots of the equation $\phi(z,t) = E_z$.

Consider particle motion starting in an initial potential $\phi(z)$ that slowly evolves in time toward a final potential $\phi'(z) = \phi(z) + \delta\phi(z)$. Under this evolution, the axial energy E_z changes to E_z', and the adiabatic invariant evolves in functional form from $J(E_z)$ to $J'(E_z')$ where

$$J(E_z) = 2\int_{z_1}^{z_2} \sqrt{2m[E_z - \phi(z)]}dz, \tag{2}$$

$$J'(E_z') = 2\int_{z_1'}^{z_2'} \sqrt{2m\left[E_z' - \phi'(z)\right]}dz. \tag{3}$$

In Eq. (3), the primes on the turning points indicate that they have moved due to the change in energy and potential.

According to the theory of adiabatic invariance, the value of the invariant is unchanged under this evolution

$$J'(E_z') = J(E_z); \tag{4}$$

in other words, the phase-space area of the initial orbit is the same as that of the final orbit. This equation, together with Eqs. (2) and (3), allows one to determine the final energy E_z' in terms of the initial energy E_z.

An explicit formula for the energy change can be found when the change in potential $\delta\phi(z)$ is small. Defining $\delta E_z = E_z' - E_z$ and Taylor expanding Eq. (3) to first order in small δE_z and $\delta\phi$ yield

$$J'(E_z') = 2m\int_{z_1'}^{z_2'} V_z(E_z,z)dz + 2\int_{z_1'}^{z_2'} \frac{\delta E_z - \delta\phi(z)}{V_z(E_z,z)}dz, \tag{5}$$

where

$$V_z(E_z,z) = \sqrt{2(E_z - \phi(z))/m} \tag{6}$$

is the particle speed as a function of position, for given energy E_z. Note that, although $V_z(E_z,z)$ approaches zero at the end points of the integration, this Taylor expansion to first order is still allowed because the integral in the second line is integrable (provided $E_z \neq \phi_s$, the separatrix energy). In the second integral, z_1' and z_2' can be replaced by z_1 and z_2, respectively, because the difference between the primed and unprimed turning points is small, and the integral is already small. In the first integral, one can make the same replacements because the integrand vanishes at $z = z_1$ and $z = z_2$, so that small variations in the turning points produce changes in the integral value only at the second order in their variation. Therefore, to the first order in $\delta\phi$, the first integral equals $J(E_z)$ [see Eq. (2)], and Eq. (5) can then be expressed as

$$J'(E_z') = J(E_z) + 2\int_{z_1}^{z_2} \frac{\delta E_z - \delta\phi(z)}{V_z(E_z,z)}dz. \tag{7}$$

However, according to Eq. (4), the adiabatic invariant is unchanged, so the integral in Eq. (7) must equal zero. Rearranging terms then implies that the energy change during the evolution is given by

$$\delta E_z = \langle \delta\phi \rangle \equiv \frac{2}{\tau}\int_{z_1}^{z_2} \frac{\delta\phi(z)}{V_z(E_z,z)}dz, \tag{8}$$

where $\langle\rangle$ is the "bounce-average" operation, a time-average along the orbit, τ is the orbit period

$$\tau(E_z) = 2\int_{z_1}^{z_2} \frac{dz}{V_z(E_z,z)}, \tag{9}$$

and $\langle\delta\phi\rangle(E_z)$ is the bounce-averaged change in the potential, averaged over a particle orbit of energy E_z.

Equation (8) can also be obtained directly from the Hamiltonian equations of motion of a particle in a time-varying potential. These equations imply that the time rate of change of the particle's energy is determined by the explicit time-variation in the potential according to

$$\frac{dE_z}{dt} = \frac{\partial\phi}{\partial t}. \tag{10}$$

Integrating both sides from the initial to final time yields

$$\delta E_z = \int_{t_i}^{t_f} dt(\partial\phi(z,t)/\partial t)|_{z=z(t)}. \tag{11}$$

Noting that $z(t)$ oscillates rapidly as particles bounce between turning points allows one to replace the integrand by its bounce average, yielding $\delta E_z = \int_{t_i}^{t_f} dt\partial\langle\phi\rangle/\partial t$. Performing the time integral then returns us to Eq. (8).

A. Adiabatic change in the particle distribution function

We now turn to a description of the collisionless evolution of a distribution of particles as the potential slowly varies in time. Consider a band of particles in phase space moving in the initial potential $\phi(z)$, and uniformly distributed between action values J and $J+dJ$. The distribution function for this band of particles is the phase space density f, i.e., fdJ is the number of particles in the band. Now, as the potential evolves to $\phi'(z)$, the band of particles evolves to a new band, but the area of the band is unchanged since this area is an adiabatic invariant. Since the number of particles is also unchanged, the final phase space density in the band, f', must equal the initial density f. If one considers the distribution to be a function of energy, this result can be expressed as

$$f'(E_z') = f(E_z), \tag{12}$$

which accounts for the fact that the energy of the particles changes from E_z to E_z' during the evolution.

When the potential changes by only a small amount $\delta\phi$, an explicit expression for the change in the distribution function can be obtained. We first express Eq. (12) as

$$f'(E_z') = f(E_z' - \delta E_z), \tag{13}$$

then Taylor expand, and apply Eq. (8) to obtain

$$f'(E_z') = f(E_z') - \langle\delta\phi\rangle\partial f/\partial E_z'. \tag{14}$$

The new distribution can be written explicitly in terms of coordinates and velocities since $E_z'(z,v_z) = \frac{1}{2}mv_z^2 + \phi'(z)$ and $\phi' = \phi + \delta\phi$

$$\begin{aligned} f'(z,v_z) &= f(E_z(z,v_z) + \delta\phi(z)) - \langle\delta\phi\rangle\partial f/\partial E_z', \\ &= f(E_z(z,v_z)) + [\delta\phi(z) - \langle\delta\phi\rangle]\partial f/\partial E_z, \end{aligned} \tag{15}$$

where, in the second line, the distribution is Taylor expanded and the prime on the partial derivative with respect to energy is dropped because the difference is second order in the variation. Thus, at a fixed phase space coordinate (z,v_z), the adiabatic first-order change δf in the distribution function is

$$\delta f(z,v_z) = [\delta\phi(z) - \langle\delta\phi\rangle]\partial f/\partial E_z. \tag{16}$$

When the initial distribution function f is a Maxwellian at temperature T, Eq. (16) simplifies to

$$\delta f(z,v_z) = -\frac{\delta\phi(z) - \langle\delta\phi\rangle}{T}f. \tag{17}$$

The term $-\delta\phi$ gives the Boltzmann response to a potential perturbation (modulo, an additive constant required to conserve particles on a field line), the expected response once collisions relax the plasma to a local thermal equilibrium state. The term $\langle\delta\phi\rangle$ is required in the *collisionless* plasma response to the potential in order that the number of particles on every energy surface is conserved in the adiabatic process, as required in Vlasov dynamics. Conservation of particle number on every energy surface can be proven by taking the bounce-average of the right hand side of Eq. (17), which averages over the energy surface chosen for the bounce-average

$$\langle(\delta\phi(z) - \langle\delta\phi\rangle)f\rangle = (\langle\delta\phi\rangle - \langle\delta\phi\rangle)f = 0. \tag{18}$$

B. Phase-space discontinuities from a squeeze potential

When the equilibrium potential $\phi(z)$ has an applied "squeeze" (i.e., a local potential maximum within the plasma, separating two regions of trapped particles on each side of the maximum), the adiabatic first-order change in the particle distribution $\delta f(z,v_z)$ will exhibit discontinuities. (We are again suppressing radial dependences for notational convenience.) These discontinuities are caused by the difference in the response of trapped and passing particles to the change in the potential, $\delta\phi(z)$.

As a simple example, consider particles confined by reflecting walls at locations $z=0$ and $z=L$. A squeeze potential of height ϕ_s is applied at $z=L_1$ and is assumed to be very narrow in z so that it produces specular reflection of trapped particles with kinetic energies less than ϕ_s, but has no effect on passing particles with kinetic energies larger than ϕ_s. This plasma model approximates the situation in experiments for which the Debye length is very small compared with the plasma length, causing applied potentials to be z-independent within the plasma, except in Debye sheaths

at the squeeze and at the plasma ends. Particle reflection off of the rapidly varying potential in the Debye sheath then approximates the effect of a reflecting wall.

Now consider the effect of the small potential perturbation that occurs when the end walls at $z=0$ and $z=L$ are slowly moved to $z=\delta L_1$ and $z=L-\delta L_2$, respectively (note the minus sign in the second case). Let us first neglect the effect of self-generated potentials. For trapped particles to the left of the squeeze, the particle density and energy increase since the region they are trapped in decreases in length by δL_1, and to the right of the squeeze, the density and energy of trapped particles increase by a different amount as that region compresses by δL_2, and for passing particles, the density and energy increase by different amounts, as the plasma compresses by $\delta L_1+\delta L_2$. For instance, if $\delta L_2=-\delta L_1$ (the case of interest in our experiments), the passing particles' energy is unchanged (in adiabatic theory).

In more detail, the energy change for trapped particles to the left due to the 1 D adiabatic compression is $\delta E_z = mv_z^2\delta L_1/L_1$, and to the right, $\delta E_z = mv_z^2\delta L_2/L_2$ where $L_2=L-L_1$, and for passing particles $\delta E_z = mv_z^2(\delta L_1+\delta L_2)/L$. Then according to Eq. (13) (after Taylor-expanding, and assuming that f is a Maxwellian), the trapped particle distribution function to the left and the right of the squeeze is

$$\delta f=\begin{cases}\dfrac{mv_z^2\delta L_1}{TL_1}f, & v_z^2<2\phi_s/m \ \&\ z<L_1\\ \dfrac{mv_z^2\delta L_2}{TL_2}f, & v_z^2<2\phi_s/m \ \&\ z>L_1\end{cases} \tag{19}$$

for trapped particles to the left (right) of the squeeze, while for passing particles

$$\delta f=\frac{mv_z^2(\delta L_1+\delta L_2)}{TL}f, \quad v_z^2>2\phi_s/m. \tag{20}$$

Thus, a discontinuity develops in the perturbed distribution at the separatrix between passing and trapped particles, which is at $v_z^2=2\phi_s/m$.

Equations (19) and (20) also follow from Eq. (17). For a "reflecting wall" with potential $\phi(z)$ that is zero away from $z=0$, that rises rapidly at $z=0$ so as to cause reflections, and that moves in z by δL_1, the perturbed potential is of the form $\delta\phi=\phi(z-\delta L_1)-\phi(z)$. Taylor expansion then implies $\delta\phi=-\delta L_1\partial\phi/\partial z$. This implies that $\delta\phi=0$ away from the wall at $z=0$, but $\langle\delta\phi\rangle\neq 0$. For particles trapped to the left of the squeeze, i.e., between a moving wall at $z=0$ and the squeeze at $z=L_1$, the bounce-averaged potential is

$$\begin{aligned}\langle\delta\phi\rangle &= \frac{2}{\tau}\int_{z_1}^{L_1}\frac{dz}{V_z(E_z,z)}\delta\phi(z)=-\frac{2\delta L_1}{\tau}\int_{z_1}^{L_1}\frac{dz}{V_z(E_z,z)}\frac{\partial\phi}{\partial z}\\ &= \frac{2m\delta L_1}{\tau}\int_{z_1}^{L_1}dz\frac{\partial}{\partial z}V_z(E_z,z)=\frac{2\delta L_1}{\tau}\left(\sqrt{2mE_z}-0\right)\\ &= mv_z^2\delta L_1/L_1,\end{aligned} \tag{21}$$

where we used Eq. (6) in the second line, and $\tau=2L_1/|v_z|$ for left-trapped particles. Similar arguments can be used to obtain the bounce-averaged perturbed potential in the right-trapped and passing regions.

Note that the Taylor expansion of $\phi(z-\delta L_1)$ used to derive Eq. (21) requires that δL_1 be small compared with the minimum scale length of variation of $\phi(z)$, which we define as λ. (In experiments,[12] λ is of order the Debye length.) For a rapidly varying "reflecting wall" potential with $\lambda\ll L_1$, the condition $\delta L_1\ll\lambda$ is a stringent requirement on δL_1. This requirement is a limitation of the linearization approach used to derive Eq. (17). Nevertheless, this equation allows us to obtain the perturbed distribution function everywhere in the plasma to linear order in δL_1, including at the plasma ends where $\phi(z)$ varies on the scale of λ. On the other hand, Eqs. (19) and (20) were derived assuming that $\delta L_1\ll L_1$, a less stringent requirement on δL_1. However, Eqs. (19) and (20) do not hold throughout the plasma. They are incorrect in the Debye sheaths at the plasma ends where $\phi(z)$ is varying rapidly: they do not display the density changes in the ends depicted by $+/-$ symbols in Fig. 1, while Eq. (17) does so through the term $\delta\phi(z)$, which is not included in Eq. (19) or (20).

It is interesting that both approaches to the above "reflecting wall" problem give the same result for δf away from the ends of the plasma, suggesting that Eq. (17) may be useful in the central region of the plasma, away from the ends, even for end motions that are larger than λ. This is a hopeful sign for the linear theory, since it might still apply to experiments now being conducted[12] that typically operate with $\delta L>\lambda$.

However, the perturbed distribution function is modified by the self-consistent plasma potential, which is not included in Eq. (19) or (20). The density changes associated with the compressions/expansions produce a self-consistent potential change $\delta\phi_p$. This self-consistent potential change is often of the same order of magnitude as the external potential change, and therefore must be taken into account.

For a long plasma column, the potential change on the left side is independent of z away from the ends and the squeeze, i.e., for $0<z<L_1$ (due to Debye-shielding). The potential then changes sign in the squeeze region and again becomes independent of z on the right side in the range $L_1<z<L$. This implies that, for trapped particles, the self-consistent potential change satisfies $\langle\delta\phi_p\rangle=\delta\phi_p$, and so, according to Eq. (17), the trapped particle distribution is unaffected by the self-consistent plasma potential.

However, for passing particles, $\langle\delta\phi_p\rangle\neq\delta\phi_p$ and so Eqs. (17) and (20) imply

$$\delta f=\frac{mv_z^2(\delta L_1+\delta L_2)}{TL}f-\frac{(\delta\phi_p-\langle\delta\phi_p\rangle)}{T}f, \quad v_z^2>2\phi_s/m. \tag{22}$$

The self-consistent potential can then be found using Poisson's equation. Defining $\delta\phi_{p,1}(r)$ and $\delta\phi_{p,2}(r)$ as the self-consistent potential perturbation on the left and right sides, respectively, the Poisson equation for each side is

$$\nabla_r^2\delta\phi_{p,j}=-4\pi q^2\delta n_j, \tag{23}$$

where $j=1, 2$, $\nabla_r^2 = 1/r(\partial/\partial r)r(\partial/\partial r)$, and where δn_j is the density perturbation on side j, given by the velocity integral of the perturbed distribution functions, Eqs. (19) and (22)

$$\delta n_j = 2\frac{\delta L_j}{L_j} n \int_0^{\sqrt{2\phi_s/m}} dv_z \frac{mv_z^2}{T}\frac{e^{-mv_z^2/2T}}{\sqrt{2\pi T/m}} - 2n \int_{\sqrt{2\phi_s/m}}^{\infty} dv_z e^{-mv_z^2/2T} \times \frac{\delta\phi_{p,j} - \langle\delta\phi_p\rangle - mv_z^2(\delta L_1 + \delta L_2)/L}{T\sqrt{2\pi T/m}}. \quad (24)$$

The first integral in Eq. (24) is the contribution $\delta n_{j,T}$ to the perturbed density from trapped particles, and the second is the contribution from passing particles, $\delta n_{j,P}$. These integrals can each be performed analytically

$$\delta n_{j,T} = n\frac{\delta L_j}{L_j}(\eta_T - \Delta\eta),$$
$$\delta n_{j,P} = n\frac{\delta L_1 + \delta L_2}{L}(\eta_P + \Delta\eta) - n\frac{\delta\phi_{p,j} - \langle\delta\phi_p\rangle}{T}\eta_P, \quad (25)$$

where $\eta_T = \mathrm{erf}\left(\sqrt{\phi_s/T}\right)$ is the equilibrium fraction of trapped particles, $\eta_P = 1 - \eta_T = \mathrm{erfc}\left(\sqrt{\phi_s/T}\right)$ is the equilibrium fraction of passing particles, and $\Delta\eta = 2\sqrt{\frac{\phi_s}{\pi T}}e^{-\phi_s/T}$ is the change in these fractions caused by particles going from trapped to passing and passing to trapped as the plasma length varies.

For the passing particles, the term proportional to $\delta\phi_{p,j} - \langle\delta\phi_p\rangle$ describes the density change due to Debye-shielding. The η_P factor arises because only passing particles can move from end to end to Debye-shield the potential created by the trapped particles. The term proportional to $\delta L_1 + \delta L_2$ is the density change of the passing particles due to the overall change in plasma length. Here, the factor $\Delta\eta$ arises from particles that go from trapped to passing during the adiabatic energy increase caused by the length change (when $\delta L_1 + \delta L_2 > 0$, the plasma length decreases). For the trapped particles, the equilibrium fraction η_T is also modified by $\Delta\eta$ because some particles become untrapped during compression. These particles either become passing or are retrapped on the other side. For example, if $\delta L_2 = -\delta L_1$, all particles that become untrapped on the left side are retrapped on the right side; none become passing.

Equations (23) and (25) can be simplified by noting that, for the passing particles, the bounce averaged potential in Eq. (25) is $\langle\delta\phi_p\rangle = (L_1\delta\phi_{p,1} + L_2\delta\phi_{p,2})/L$. Acting on this expression with ∇_r^2, neglecting radial variation in L_1/L and L_2/L (for simplicity), and using Eqs. (23) and (25) yield

$$\nabla_r^2\langle\delta\phi_p\rangle = -4\pi q^2 n\frac{\delta L_1 + \delta L_2}{L}. \quad (26)$$

Thus, the bounce-averaged potential change is only due to the overall change in the plasma length. In particular, if $\delta L_2 = -\delta L_1$, the length does not change and there is no change in the bounce-averaged potential.

The solution of Eq. (26) can then be used for $\langle\delta\phi_p\rangle$ in Eq. (25). This allows solution of Eq. (23) on each side separately. The equation is most easily expressed in terms of the scaled potential difference $\psi_j(r)$, defined by the expression $\delta\phi_{p,j} - \langle\delta\phi_p\rangle \equiv \psi_j T$

$$\nabla_r^2\psi_j = \frac{4\pi q^2 n}{T}\left[\psi_j\eta_P - \frac{\Delta L_j}{L_j}(\eta_T - \Delta\eta)\right], \quad (27)$$

where the scaled length change on each side j, ΔL_j, is given by

$$\Delta L_j = \frac{\delta L_j L_k - \delta L_k L_j}{L}, \quad (28)$$

with $j \neq k$. For instance, if $\delta L_1 = -\delta L_2 = \delta L$, then $\Delta L_j = \delta L_j$. The first term in the square bracket of Eq. (27) is the Debye-shielding density change due to passing particles, and the second term is the density change due to trapped particles, which acts as an inhomogeneous term in the differential equation.

Equations (26) and (27) can be solved numerically (e.g., via the shooting method) for the radial dependence of the perturbed potential on each side of the squeeze. These equations are useful for a long thin plasma column with a short (in z) applied squeeze potential. In Sec. II C we consider general expressions for the self-consistent potential change, applicable to realistic plasmas with an applied squeeze.

C. Self-consistent effects

In this section, we derive a general expression for the change in the self-consistent potential from an external potential that changes adiabatically. The total potential change $\delta\phi$ can be broken into a portion $\delta\phi_{ext}$ produced externally by variation of voltages on external electrodes, and a portion $\delta\phi_p$ produced by the plasma response to the external potential variation: $\delta\phi = \delta\phi_{ext} + \delta\phi_p$. The external potential is a solution of Laplace's equation, $\nabla^2\delta\phi_{ext} = 0$, depending only on boundary conditions given by the voltage change on the electrodes. In contrast, the plasma potential satisfies Poisson's equation

$$\nabla^2\delta\phi_p = -4\pi q^2\int dv_z\delta f(r, z, v_z), \quad (29)$$

with boundary conditions that $\delta\phi_p = 0$ on the surrounding electrodes. Since δf depends implicitly on $\delta\phi_p$, this self-consistent equation for $\delta\phi_p$ is harder to solve. Nevertheless, $\delta\phi_p$ cannot simply be neglected because it is often of the same magnitude as $\delta\phi_{ext}$.

Assuming that the initial distribution function f is of Boltzmann form in z and v_z, i.e., $f = N(r)\exp[-E_z/T]$, where $N(r)$ is any function of r, the perturbed distribution function δf is given by Eq. (17) which leads to

$$\nabla^2\delta\phi_p = \frac{4\pi q^2 n}{T}\left(\delta\phi_p + \delta\phi_{ext} - \int dv_z\frac{e^{-mv_z^2/2T}}{\sqrt{2\pi T/m}}\langle\delta\phi_p + \delta\phi_{ext}\rangle\right), \quad (30)$$

where $n(r, z) = N(r)e^{-\phi(r,z)/T}\sqrt{2\pi T/m}$ is the initial plasma number density. For a given external potential perturbation

$\delta\phi_{ext}(r,z)$, Eq. (30) is an inhomogeneous linear integro-differential equation for the perturbed plasma potential $\delta\phi_p(r,z)$. The equation is nonlocal in z due to the appearance of the bounce-average operator $\langle\,\rangle$. The nonlocality can be seen explicitly by substituting the form of the bounce-average operator into Eq. (30) [see Eq. (8)]

$$\nabla^2\delta\phi_p = \frac{4\pi q^2 n}{T}\left(\delta\phi_p(r,z)+\delta\phi_{ext}(r,z) - \int dv_z \frac{e^{-mv_z^2/2T}}{\sqrt{2\pi T/m}} \times \frac{2}{\tau(E_z,r)} \int_{z_1(E_z,r)}^{z_2(E_z,r)} \frac{dz'}{V_z(E_z,z')}\left[\delta\phi_p(r,z')+\delta\phi_{ext}(r,z')\right]\right), \tag{31}$$

where, in the velocity integrations, we must remember that energy E_z depends on v_z as $E_z = mv_z^2/2 + \phi(r,z)$.

D. Self-consistent evaluation of the perturbed adiabatic plasma potential

In this section, we describe the numerical results that solve Eq. (31) for the self-consistent perturbed potential in realistic geometry. In current experiments, this full solution is required because the plasma is not sufficiently long and the squeeze region is not sufficiently narrow to make Eq. (27) a good approximation. The method employed in the solution is discussed in Appendix A. The method solves the integro-differential equation (31) on a radial and axial grid for a given plasma equilibrium and a given perturbed external potential due to voltage changes applied to the cylindrical end electrodes.

In Fig. 2(a), the contour plot of the equilibrium density $n(r, z)$ is displayed for a typical nonneutral plasma with a temperature of $T = 0.45$ eV, computed using standard techniques[20] in a cylindrical Penning-Malmberg trap geometry. Here, $L_0 = 23.24$ cm is the length scale of the computation volume, and the density is measured in units of 10^6cm^3. The plasma is confined axially by 100 eV potentials applied to cylindrical electrodes at each end, and a squeeze potential of 15 eV is applied to a cylindrical electrode that runs from $z = 0.5L_0$ to $z = 0.65L_0$. The cylindrical electrode radii are 2.86 cm, and the plasma radius is roughly 0.7 cm, although this varies with z considerably due to the applied squeeze potential.

In Fig. 3(a), contour plot of the perturbed density $\delta n(r,z)$ is displayed, computed by solving Eq. (31) using the numerical method described in Appendix A, using 401 axial grid points and 128 radial grid points. (It may be useful to compare this with the schematic in Fig. 1.) This is the collisionless adiabatic density response to a change in the left and right electrode potentials of $+\delta V$ and $-\delta V$, respectively, where $\delta V = 10$ eV (i.e., 10% changes in the 100 eV end potentials). The plasma moves to the right due to this wall voltage change, implying a relatively large positive density change on the right plasma end and a negative density change at the left end. Away from the ends, and at larger radii near the radial plasma edge, most particles are trapped by the squeeze potential, and so the plasma density increases on the left side and decreases on the right side as the trapped particles are compressed on the left and expanded on the right. However, at smaller radii, most particles are able pass through because the Debye-shielded squeeze potential is considerably smaller, and here, the plasma density response changes sign as these passing particles Debye-shield the trapped particle response at larger radii. This behavior has been shown schematically in Fig. 1 by the + and –signs.

Figure 4 displays the bounce-averaged perturbed potential $\langle\delta\phi\rangle(E_z,r)$ computed at radius $r/L_0 = 0.63\,\text{cm}/23.24\,\text{cm} = 0.027$ for a particle with energy E_z, plotted as a function of E_z. This potential is positive for particles trapped on the left side of the squeeze potential, where the plasma has been compressed by the applied electrode potential change δV. On the right side, the plasma response is opposite in sign for the trapped particles. On each side, Debye-shielding arising from the plasma potential $\delta\phi_p$ reduces the size of $\langle\delta\phi\rangle$ by about

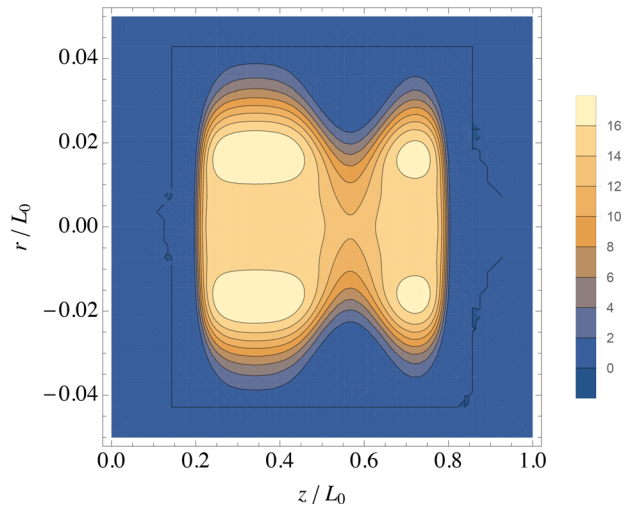

FIG. 2. Equilibrium density contours (in units of 10^6cm^3) in a $T = 0.45$ eV plasma to which a 15 eV squeeze potential is applied to a cylindrical electrode just to the right of the plasma center. Here, $L_0 = 23.24$ cm, and the electrode radius is 2.86 cm.

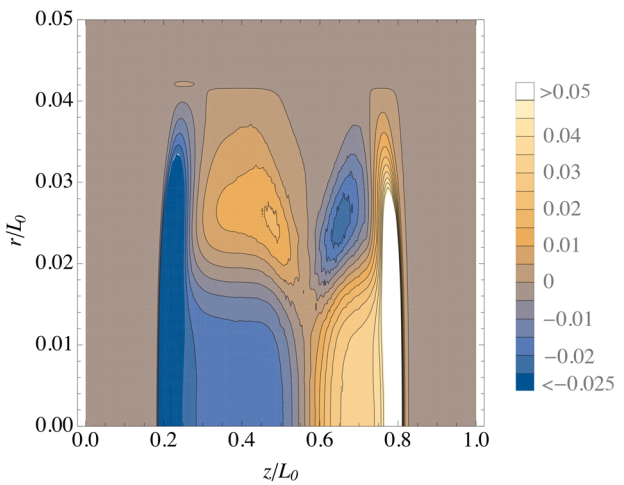

FIG. 3. Adiabatic density response divided by the central density, $\delta n(r,z)/n(r=0,z=L_0/2)$, due to an end potential perturbation of +10 eV on the left and −10 eV on the right.

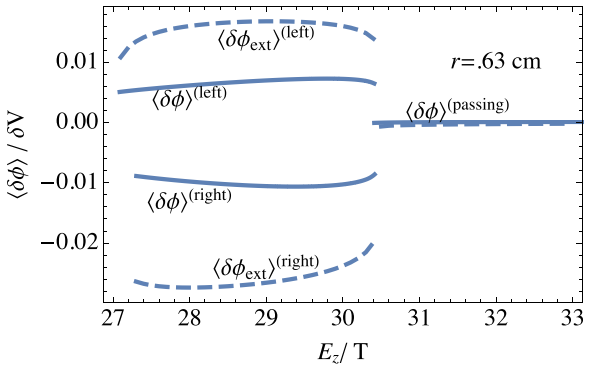

FIG. 4. Solid lines: Bounce-averaged perturbed potential $\langle\delta\phi\rangle$ for a particle with energy E_z, plotted versus E_z, at radius $r = 0.63$ cm ($r/L_0 = 0.027$). Dashed lines: Bounce-averaged external potential $\langle\delta\phi_{ext}\rangle$. The potentials are scaled to the applied end potential perturbation δV.

a factor of 2 compared with the bounce-averaged external potential perturbation $\langle\delta\phi_{ext}\rangle$ (the dashed lines). For the passing particles, which average over the potential on the left and right sides, the bounce-average of the perturbed potential is almost zero. The minimum energies plotted, roughly $27T = 12$ eV, arise from the minimum values of the equilibrium plasma potential at this radius (with a slightly different minimum value on the left and right sides). The plot shows that particles with kinetic energies up to about $3T = 1.4$ eV are trapped at this fairly large radius; in other words, almost all particles are trapped.

Figure 5 displays the bounce-averaged perturbed potentials plotted versus energy at a series of radii. The plot shows that at all radii $\langle\delta\phi\rangle \sim 0$ for passing particles, $\langle\delta\phi\rangle > 0$ for left-trapped particles (when $\delta V > 0$), and $\langle\delta\phi\rangle < 0$ for right-trapped particles. At radii near $r = 0$, the range of energies over which particles are trapped is small, roughly $0.3T$, centered at the plasma potential $E_z \sim 35T$. However, at larger radii, the range of energies over which particles are trapped increases because the height ϕ_s of the squeeze potential barrier increases with increasing radius. Thus, the fraction of trapped particles η_T is an increasing function of radius. One can also see that the minimum potential energy for a particle at a given radius decreases with increasing radius, from

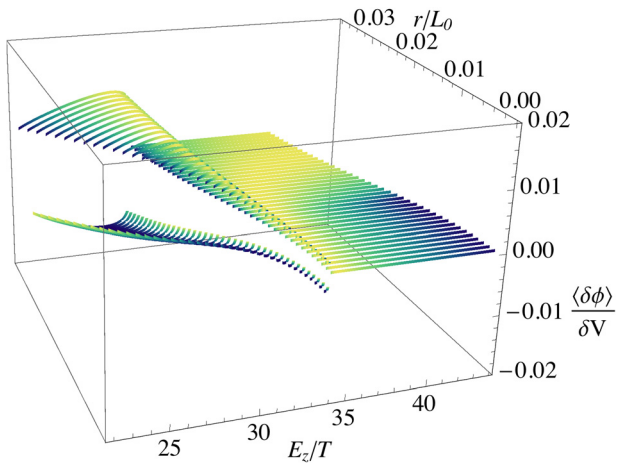

FIG. 5. Bounce-averaged perturbed potential versus energy E_z at several radii within the plasma.

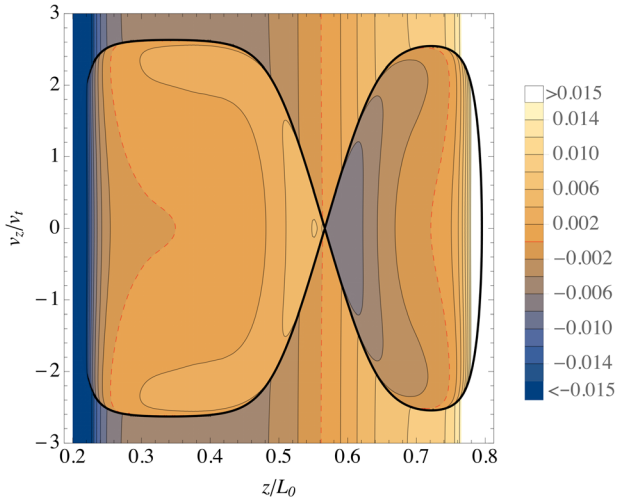

FIG. 6. Contour plot in axial position and velocity of $\delta fT/(f\delta V)$, where δf is the perturbed adiabatic distribution function [Eq. (17)] at radius $r = 0.63$ cm, f is the equilibrium distribution function at that radius, and δV is the perturbed end potential. Velocities are scaled to $v_t = \sqrt{T/m}$, the thermal speed, and positions to $L_0 = 23.24$ cm. The dashed curve is the zero contour. Note the discontinuity at the separatrix energy given by the solid black curve.

about $35T$ at $r = 0$ to about $22T$ at the plasma edge, due to the fall-off with radius in the self-consistent equilibrium plasma potential.

The discontinuity in the bounce-averaged perturbed potential $\langle\delta\phi\rangle$ produces a discontinuity in the perturbed distribution function δf [see Eq. (17)]. In Fig. 6, the perturbed distribution function at radius $r = 0.63$ cm is plotted versus z and v_z. The distribution is divided by the equilibrium distribution f in order to emphasize large velocities where the discontinuity is more noticeable. The separatrix at energy $E_z = \phi_s$ forms a "figure eight" curve and the discontinuity in δf along this curve is apparent as an abrupt shift in the contours. In Fig. 7, the perturbed distribution is displayed versus velocity at two values of z and at the same radius as in Fig. 6. At $z/L_0 = 0.35$, a location chosen well away from the plasma ends, and from the squeeze, the distribution is close to that given by the simplified model of Eqs. (19) and (22): $\delta f/f$ is roughly quadratic in v_z for trapped particles and nearly constant in v_z for passing particles (when $\delta L_2 = -\delta L_1$). However, at $z/L_0 = 0.5$, nearer the squeeze region, the perturbed distribution function deviates significantly from the simplified model.

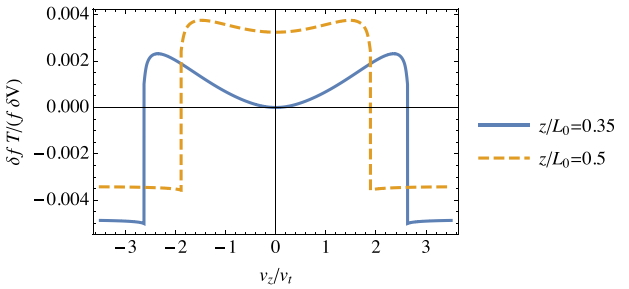

FIG. 7. Plots of $\delta fT/(f\delta V)$ versus velocity at two axial positions, at radius $r = 0.63$ cm.

III. COLLISIONS AND HEATING

In this section, we consider the effect of interparticle collisions on the perturbed velocity distribution, focusing on the effect of collisions on the discontinuity in the distribution function at the separatrix between trapped and passing particles. In the $\sqrt{\nu}$ regime where $\nu \ll \omega \ll \omega_b$, collisions smooth out this discontinuity, producing a narrow collisional boundary layer at the separatrix, where particles are able to randomly detrap and retrap, causing entropy production and heating. The width of this boundary layer scales with collisionality as $\sqrt{\nu}$, and so does the heating rate.

When collisions are added to the equations of motion, we assume that the perturbed distribution function δf evolves according to a Fokker-Planck equation

$$\frac{\partial \delta f}{\partial t} + v_z \frac{\partial \delta f}{\partial z} - \frac{1}{m}\frac{\partial \phi}{\partial z}\frac{\partial \delta f}{\partial v_z} - \frac{1}{m}\frac{\partial \delta\phi}{\partial z}\frac{\partial f}{\partial v_z} = \frac{T}{m}\frac{\partial}{\partial v_z}\nu\left(\frac{\partial \delta f}{\partial v_z} + \frac{m v_z}{T}\delta f\right). \tag{32}$$

The simple collision operator used here is sufficient to describe the collisional boundary layer in the $\sqrt{\nu}$ regime. The collision frequency ν can be regarded as a function of particle energy and position.

To describe the effect of collisions, we break δf into two pieces

$$\delta f = f(-\delta\phi + g)/T. \tag{33}$$

The first term $-f\delta\phi/T$ represents the linearized Boltzmann response to the perturbed potential, and the second term fg/T is a correction to this response. Applying Eq. (33) to (32), we find that the function g satisfies

$$\frac{\partial g}{\partial t} + v_z\frac{\partial g}{\partial z} - \frac{1}{m}\frac{\partial \phi}{\partial z}\frac{\partial g}{\partial v_z} = \frac{T}{m}\left(\frac{\partial}{\partial v_z}\nu\frac{\partial g}{\partial v_z} - \frac{m\nu v_z}{T}\frac{\partial g}{\partial v_z}\right) + \frac{\partial \delta\phi}{\partial t}. \tag{34}$$

This equation can be solved in the passing and trapped regions and the result patched together at the separatrix so as to produce a continuous solution for g whose first derivative is also continuous. This has been done previously for a special case, as in Ref. 21. Here, we note that the largest collisional effect is the smoothing of the discontinuity in the energy of the bounce-averaged (adiabatic) distribution function, and so we consider only the bounce averaged portion of this equation, which dominates the plasma response in the regime of interest, $\nu \ll \omega \ll \omega_b$.

We first replace $g(z, v_z, t)$ by its bounce average $\langle g\rangle(E_z, t)$. We then bounce-integrate the equation, acting on both sides with $\oint dz/v_z$, where the integral is along a collisionless orbit for which energy E_z is fixed. The integral of the collision operator is simplified by noting that $\partial/\partial v_z|_z = m v_z \partial/\partial E_z|_z$. We also keep only the second-derivative term in the collision operator since this dominates in the boundary layer where the solution for $\langle g\rangle$ varies rapidly with E_z. The result is

$$\tau\frac{\partial\langle g\rangle}{\partial t} = \langle\nu\rangle JT\frac{\partial^2\langle g\rangle}{\partial E_z^2} + \tau\frac{\partial\langle\delta\phi\rangle}{\partial t}, \tag{35}$$

where $\langle\nu\rangle = \oint dz m v_z \nu/J$ is the bounce-averaged collision rate. Dividing by τ, we arrive at

$$\frac{\partial\langle g\rangle}{\partial t} = \nu_E T^2\frac{\partial^2\langle g\rangle}{\partial E_z^2} + \frac{\partial\langle\delta\phi\rangle}{\partial t}, \tag{36}$$

where ν_E is the energy diffusion rate, given by $\nu_E \equiv \langle\nu\rangle J/\tau T$. Similar bounce-averaged energy diffusion equations for the distribution function have been derived previously in association with cross-field transport and diocotron-mode damping.[4,15] This particular form is somewhat simpler because it does not require azimuthal plasma motion. It is also more general in that it is correct for arbitrary squeeze potentials; the previous derivations assumed a long thin plasma and a narrow squeeze region.

In Eq. (36), $\langle\delta\phi\rangle$ changes discontinuously at the energy separatrix (see Fig. 4), taking values $\langle\delta\phi\rangle^{(P)}$ in the passing region $E_z > \phi_s$ and $\langle\delta\phi\rangle^{(L,R)}$ in the left and right trapped regions respectively, where $E_z < \phi_s$. However, near the separatrix, within the collisional boundary layer on each side of the separatrix, we can treat these bounce-averaged functions as constants, independent of energy since the boundary layer is narrow; also, ν_E can be treated as constant in the boundary layer, but taking different values $\nu_E^{(j)}$ in the different regions (because $\langle\nu\rangle$, J and τ differ in each region). Then, assuming time-dependence of the form $\langle g\rangle = \mathrm{Re}\langle g\rangle^{(j)}e^{-i\omega t}$ and $\langle\delta\phi\rangle = \mathrm{Re}\langle\delta\phi\rangle^{(j)}e^{-i\omega t}$ in each region j, the general solution of Eq. (36) is

$$\langle g\rangle^{(j)} = A^{(j)}e^{\alpha^{(j)}(E_z-\phi_s)/T} + B^{(j)}e^{-\alpha^{(j)}(E_z-\phi_s)/T} + \langle\delta\phi\rangle^{(j)}, \tag{37}$$

where $\alpha^{(j)} = (1-i)\sqrt{\omega/2\nu_E^{(j)}}$, and $A^{(j)}$ and $B^{(j)}$ are undetermined coefficients. We take $B^{(L)} = B^{(R)} = A^{(P)} = 0$ so that the solutions in the trapped and passing regions do not blow up. With these choices, the solutions match the collisionless solution $\langle\delta\phi\rangle^{(j)}$ in each region for energies far from the separatrix energy ϕ_s. The values of the remaining undetermined coefficients are connected by the condition that the distribution be continuous across the separatrix, which implies

$$\begin{aligned}\langle g\rangle^{(R,L)} &= (g_s - \langle\delta\phi\rangle^{(R,L)})e^{\alpha^{(R,L)}(E_z-\phi_s)/T} + \langle\delta\phi\rangle^{(R,L)},\\ \langle g\rangle^{(P)} &= (g_s - \langle\delta\phi\rangle^{(P)})e^{-\alpha^{(P)}(E_z-\phi_s)/T} + \langle\delta\phi\rangle^{(P)},\end{aligned} \tag{38}$$

where g_s is the value of $\langle g\rangle^{(j)}$ on the separatrix. Finally, g_s can be determined from the condition that the total number of particles at each radius is unchanged by the perturbation: $\delta N = \int dz dv \delta f = 0$. Converting variables to (ψ, J), taking

$$\delta f = f(-\delta\phi + \langle g\rangle)/T \tag{39}$$

and noting that $\int d\psi\delta\phi = 2\pi\langle\delta\phi\rangle$ and that $dJ = dE\tau$, after integrating over the exponential boundary layer in each region, we obtain

$$\delta N = 0 = \frac{f_s}{m}\left[\frac{\tau_s^{(L)}}{\alpha^{(L)}}(g_s - \langle\delta\phi\rangle_s^{(L)}) + \frac{\tau_s^{(R)}}{\alpha^{(R)}}(g_s - \langle\delta\phi\rangle_s^{(R)}) + \frac{\tau_s^{(P)}}{\alpha^{(P)}}(g_s - \langle\delta\phi\rangle_s^{(P)})\right], \tag{40}$$

where f_s is the equilibrium distribution at the separatrix energy, $\tau_s^{(j)}$ is the bounce period in each region near the separatrix energy, and the subscript s on bounce averages indicates that they too are evaluated near the separatrix energy. Solving for g_s then yields

$$g_s = \frac{\sum_j \sqrt{\langle\nu\rangle_s^{(j)}\tau_s^{(j)}J_s^{(j)}}\langle\delta\phi\rangle_s^{(j)}}{\sum_j \sqrt{\langle\nu\rangle_s^{(j)}\tau_s^{(j)}J_s^{(j)}}}, \tag{41}$$

where we have used $\alpha^{(j)} = (1-i)\sqrt{\omega/2\nu_E^{(j)}}$ and $\nu_E = \langle\nu\rangle J/\tau T$.

Before proceeding, note that bounce averages are often singular at the separatrix energy, since the period τ approaches infinity there. However, these singularities are exponentially narrow for typical potential profiles, and we assume that this width is small compared with the width in energy of the collisional boundary layer, of order $\sqrt{T\phi_s\nu/\omega}$. In this case, the singularities are washed out by collisional diffusion, so quantities in the above expressions that are evaluated at the separatrix are actually averaged over the narrow boundary layer, and are therefore not singular.

In Fig. 8, we plot $\mathrm{Re}\langle g\rangle^{(j)}$ and $\mathrm{Im}\langle g\rangle^{(j)}$ in the passing, right-trapped, and left-trapped regions, evaluated at radius $r = 0.63$ cm using Eq. (38), and assuming that $\omega/2\nu_E^{(j)} = 100$ (the dashed lines). Far from the separatrix, $\langle g\rangle = \langle\delta\phi\rangle$, but at the separatrix, the discontinuity in the collisionless distribution function is smoothed out over the collisional boundary layer. The imaginary part is nonzero only in this layer and is of the correct sign so as to cause heating (the phase of the distribution lags that of the external potential, indicating drag on the distribution due to collisions).

A. Joule heating

The mean Joule heating per oscillation period of the forcing is given by the general expression

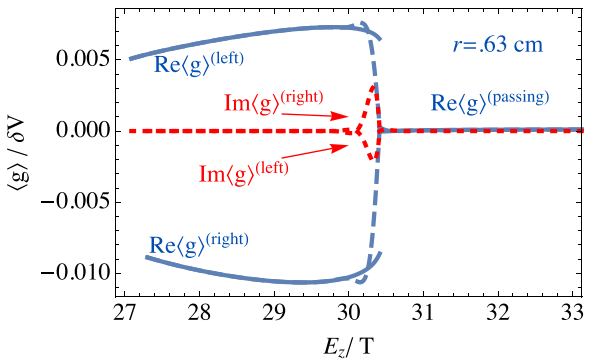

FIG. 8. Dashed and dotted lines are the functions $\mathrm{Re}\langle g\rangle^{(j)}$, and $\mathrm{Im}\langle g\rangle^{(j)}$, respectively, the real and imaginary parts of the bounce-averaged distribution function in the collisional boundary-layer analysis [see Eq. (39)], scaled by δV and evaluated at radius $r = 0.63$ cm, and plotted versus energy E_z. Solid lines are the bounce-averaged perturbed potential $\langle\delta\phi\rangle$ in collisionless theory (same as Fig. 4). The real part of $\langle g\rangle$ is in phase with the external potential and approaches $\langle\delta\phi\rangle$ away from the separatrix. The imaginary part, concentrated in the boundary layer, is 90° out of phase and is therefore responsible for heating the plasma.

$$dK/dt = -\int_0^{2\pi/\omega}\frac{\omega dt}{2\pi}\int d^3r n(r,z)\delta U_z(r,z,t)\partial\delta\phi/\partial z, \tag{42}$$

where δU_z is the perturbed fluid velocity. In order to express the integrand in terms of the perturbed density rather than the perturbed fluid velocity, we apply an integration by parts that converts the integrand to

$$\begin{aligned} dK/dt &= \int_0^{2\pi/\omega}\frac{\omega dt}{2\pi}\int d^3r\delta\phi\frac{\partial n(r,z)\delta U_z(r,z,t)}{\partial z} \\ &= -\int_0^{2\pi/\omega}\frac{\omega dt}{2\pi}\int d^3r\delta\phi(r,z,t)\partial\delta n(r,z,t)/\partial t, \end{aligned} \tag{43}$$

where, in the second line, we applied the linearized continuity equation $\partial\delta n/\partial t = -\partial(n\delta U_z)/\partial z$. This form of the Joule-heating expression can be evaluated using the perturbed distribution function via Eq. (33) (where again we consider only the bounce-averaged contribution to g)

$$\begin{aligned} dK/dt = -\int_0^{2\pi/\omega}\frac{\omega dt}{2\pi T}\int d^3r dv_z\delta\phi(r,z,t)f(r,z,v) \\ \times\left[-\delta\dot{\phi}(r,z,t) + \langle\dot{g}\rangle\right]. \end{aligned} \tag{44}$$

However, $\delta\dot{\phi}(r,z,t)$ is 90° out of phase with $\delta\phi$ and so the time integral of this portion of the expression vanishes. The result can be simplified further by noting that $dzdv_z = d\psi dJ/(2\pi m)$; that f and $\langle g\rangle$ are independent of ψ; and that $\int d\psi\delta\phi = 2\pi\mathrm{Re}[\langle\delta\phi\rangle^{(j)}e^{-i\omega t}]$

$$\begin{aligned} dK/dt = -\int_0^{2\pi/\omega}\frac{\omega dt}{2\pi mT}\int 2\pi r dr\sum_j\int_{(j)} dJf \\ \times\mathrm{Re}\left[\langle\delta\phi\rangle^{(j)}e^{-i\omega t}\right]\mathrm{Re}\left[-i\omega\langle g\rangle^{(j)}e^{-i\omega t}\right], \end{aligned} \tag{45}$$

where the sum is over separate phase-space regions (left-trapped, right-trapped, and passing), the subscript on the J integral indicates an integration over the area of the given region, and we have used $\langle\dot{g}\rangle = \mathrm{Re}[-i\omega\langle g\rangle^{(j)}e^{-i\omega t}]$ in a given region. Further simplification can be affected by using the identity

$$\int_0^{2\pi/\omega}\frac{\omega dt}{2\pi}\mathrm{Re}[ae^{-i\omega t}]\mathrm{Re}[-ibe^{-i\omega t}] = \frac{1}{2}\mathrm{Im}[a^*b], \tag{46}$$

which implies

$$dK/dt = -\frac{\omega}{2mT}\int 2\pi r dr\,\mathrm{Im}\sum_j\int_{(j)} dJf\langle\delta\phi\rangle^{(j)*}\langle g\rangle^{(j)}. \tag{47}$$

Note that the collisionless limit of Eq. (35), $\partial\langle g\rangle/\partial t = \partial\langle\delta\phi\rangle/\partial t$, implies that $\langle g\rangle = \langle\delta\phi\rangle$, which recovers the adiabatic solution for δf given by Eq. (17). In this case,

Eq. (47) implies that $dK/dt = 0$, so collisions are required in order to produce heating.

In the $\sqrt{\nu}$ regime, we can apply Eq. (38) for $\langle g\rangle^{(j)}$ to Eq. (47)

$$dK/dt = -\frac{\omega}{2mT}\int 2\pi r dr \mathrm{Im}\sum_j \int_{(j)} dE_z f \tau^{(j)} \langle\delta\phi\rangle^{(j)*} \times (g_s - \langle\delta\phi\rangle^{(j)}) e^{S^{(j)}\alpha^{(j)}(E_z-\phi_s)/T}, \quad (48)$$

where we converted the J integral to an energy integral via $dJ = \tau dE_z$, and where $S^{(j)} = 1$ in the trapped regions of phase space ($j = R$ or L) and $S^{(j)} = -1$ in the passing region ($j = P$).

The integral over E_z can now be performed assuming that the boundary layer is narrow, so that energy-dependent quantities in the integrand can be evaluated at (or near) their values on the separatrix

$$dK/dt = -\frac{\omega}{2m}\int 2\pi r dr f_s \mathrm{Im}\sum_j \frac{\tau_s^{(j)}}{\alpha^{(j)}} \langle\delta\phi\rangle_s^{(j)*} (g_s - \langle\delta\phi\rangle_s^{(j)}), \quad (49)$$

where the subscript s denotes quantities evaluated on (near) the separatrix.

According to Eq. (40), we can add to $\langle\delta\phi\rangle_s^{(j)*}$ any j-independent factor without changing the result, so we choose the factor $-g_s^*$, which implies

$$dK/dt = \frac{\omega}{2m}\int 2\pi r dr f_s \mathrm{Im}\sum_j |g_s - \langle\delta\phi\rangle_s^{(j)}|^2 \frac{\tau_s^{(j)}}{\alpha^{(j)}}. \quad (50)$$

Finally, substituting the definition of α and taking the imaginary part of the expression yield

$$dK/dt = \frac{1}{2m}\int 2\pi r dr f_s \sum_j \sqrt{\frac{\omega\langle\nu\rangle_s^{(j)} J_s^{(j)} \tau_s^{(j)}}{2T}} |g_s - \langle\delta\phi\rangle_s^{(j)}|^2, \quad (51)$$

which is manifestly positive-definite as expected for a collisional heating process that must increase the entropy of the system. We will evaluate Eq. (51) by using the collisionless adiabatic form for $\langle\delta\phi\rangle$ determined previously, neglecting the small correction due to the collisional boundary layer. This is a good approximation when $\nu/\omega \ll 1$.

Equation (51) shows that the heating rate is proportional to $\sqrt{\omega\nu}$ (provided that $\nu \ll \omega \ll \omega_b$) and is also proportional to the square of the applied perturbation potential δV since $\delta\phi$ is proportional to δV in our linear analysis. These scalings are as expected from our estimates in the Introduction.

The integrand in Eq. (51) can also be written in terms of the rate of temperature change at a given radius, $dK/dt = \int 2\pi r dr N_z(r)(3/2) dT/dt$, where $N_z(r) = \int dz n(r,z)$ is the z-integrated density. This implies that

$$dT/dt = \frac{1}{3mN_z} f_s \sum_j \sqrt{\frac{\omega\langle\nu\rangle_s^{(j)} J_s^{(j)} \tau_s^{(j)}}{2T}} |g_s - \langle\delta\phi\rangle_s^{(j)}|^2. \quad (52)$$

This local rate of temperature increase can be measured as a function of radius in experiments. The rate predicted by Eq. (52) is plotted in Fig. 9 for the plasma of Figs. 2–8, assuming that $\delta V = 10\,\mathrm{eV}$, $\omega/2\pi = 500\,\mathrm{Hz}$, and $\nu = 7.5\,\mathrm{s}^{-1}$, an appropriate value for the collision frequency in a pure Mg^+ ion plasma at the given temperature and central density of Fig. 2, and one that locates the plasma well within the $\sqrt{\nu}$ regime with $\nu \ll \omega \ll \omega_b$. The heating is peaked off-axis because the fraction of trapped particles (the dots) is larger at larger radii, but the heating also vanishes when the trapped particle fraction approaches 100% and the density falls off (see Fig. 2), because then there are few particles at the separatrix energy and the discontinuity in $\langle\delta\phi\rangle$ has a little effect. Here, the trapped particle fraction is computed as the equilibrium fraction of particles below the separatrix energy at a given radius (e.g., for $r = 0.63\,\mathrm{cm}$, the fraction of particles within the "figure eight" separatrix shown in Fig. 6).

In order to obtain a rough scaling of the heating rate with experimental parameters, it can be useful to further simplify Eq. (51) by considering the previously discussed case of a long plasma running from $0 < z < L$ with the left and right ends moving by $\delta L_1(r,t)$ and $\delta L_2(r,t)$, respectively, and with a narrow squeeze potential of height ϕ_s applied at $z = L_1$. In this case, we found the following results in Sec. II B: for passing particles $\langle\delta\phi\rangle^{(P)} = 2\phi_s(\delta L_1 + \delta L_2)/L + \langle\delta\phi_p\rangle$ where $\langle\delta\phi_p\rangle$ is the bounce-averaged perturbed plasma potential given by the solution of Eq. (26); for left-trapped particles at the separatrix energy ϕ_s, $\langle\delta\phi\rangle_s^{(L)} = 2\phi_s\delta L_1/L_1 + \delta\phi_{p,1}$, where $\delta\phi_{p,1}(r)$ is the perturbed plasma potential on the left side far from the end and from the squeeze [see Eqs. (23)–(27)]; and for right trapped particles $\langle\delta\phi\rangle_s^{(R)} = 2\phi_s\delta L_2/L_2 + \delta\phi_{p,2}$. Also, $\sqrt{J_s^{(L)}\tau_s^{(L)}} = 2\sqrt{m}L_1$, $\sqrt{J_s^{(R)}\tau_s^{(R)}} = 2\sqrt{m}L_2$, and $\sqrt{J_s^{(P)}\tau_s^{(P)}} = 2\sqrt{m}L$. These results together with Eq. (41) imply that $g_s = \langle\delta\phi\rangle^{(P)}$ and that

$$dK/dt = \sqrt{\pi\omega\nu}T\sum_{j=1,2}\int r dr n(r) e^{-\phi_s/T} L_j \left(2\frac{\Delta L_j}{L_j}\frac{\phi_s}{T} + \psi_j\right)^2, \quad (53)$$

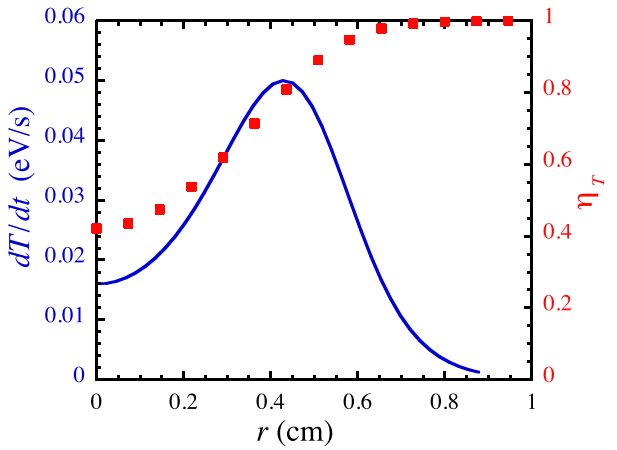

FIG. 9. Computed heating rate versus radius (solid curve; left axis scale); trapped particle fraction (dots; right axis scale).

where we have used $f_s = ne^{-\phi_s/T}/\sqrt{2\pi T/m}$, and where $\psi_j(r)$ is the scaled potential change given by the solution of Eq. (27).

When $\phi_s/T \ll 1$ in Eq. (27), $\eta_P \approx 1$ and the inhomogeneous terms can be Taylor expanded, yielding

$$\frac{1}{r}\frac{\partial}{\partial r} r \frac{\partial \psi_j}{\partial r} = \frac{4\pi q^2 n}{T}\left[\psi_j - \frac{\Delta L_j}{L_j}\frac{4\pi}{3}(\phi_s/\pi T)^{3/2}\right]. \tag{54}$$

Thus, ψ_j scales with the squeeze potential and length change as $(\Delta L_j/L_j)(\phi_s/T)^{3/2}$, and then, Eq. (53) shows that the heating rate scales as ϕ_s^2 for $\phi_s/T < 1$. This agrees with the estimate for the heating discussed in the Introduction.

IV. DISCUSSION

In this paper, we have developed theory for superbanana transport in the $\sqrt{\nu}$ regime for a simple transport process: the heating of a plasma pushed back and forth across a squeeze potential by the variation of end confinement potentials at a frequency ω chosen so that $\nu \ll \omega \ll \omega_b$. The heating is primarily due to collisional boundary-layers that build up at the separatrix between the trapped and passing particles, caused by the differing responses of the trapped and passing particles to the potential changes. The heating rate, proportional to $\sqrt{\nu\omega}$, and expressions for the nearly-discontinuous particle distribution function, will be compared with experiments in a separate paper.[12]

Entropy production scaling as $\sqrt{\nu}$ is a signature of superbanana transport predicted to occur in several magnetic confinement geometries of importance to fusion applications. The purpose of our work is to describe the processes leading to this type of transport, in a simple geometry that can be probed experimentally.

In previous works on superbanana transport that caused cross-magnetic field particle loss, it was observed that a "ruffle" on the separatrix, i.e., a θ asymmetry, could enhance the transport with a loss rate scaling as ν^0.[4,5,16–18] This enhanced transport is caused by an effective broadening of the boundary layer at the separatrix as the ruffle allows particles to chaotically trap and detrap. We believe that a similar effect could be observed in the heating process considered here. In future work, by applying a θ-asymmetry to the separatrix, we will study this chaotic heating effect in both theory and experiment.

ACKNOWLEDGMENTS

The author acknowledges useful discussions with Professor C. F. Driscoll, Dr. F. Anderegg, Dr. M. Affolter, Professor T. M. O'Neil, and D. K. Walsh. The work was supported by the NSF/DOE Partnership Grant Nos. PHY-1414570 and DE-SC0002451.

APPENDIX A: NUMERICAL METHOD

In this appendix, we describe a numerical method for the evaluation of the self-consistent perturbed plasma potential $\delta\phi_p(r,z)$ produced by an external potential change $\delta\phi_{ext}(r,z)$, via solution of the integro-differential equation Eq. (31). The homogeneous boundary conditions are that $\delta\phi_p = 0$ at the wall radius $r_w = 2.86$ cm, and that $\partial\delta\phi_p\partial z = 0$ at the two axial ends of the computational volume, $z/L_0 = 0$ and $z/L_0 = 1$.

First, we will re-order the integration over v_z and z' so that we may write Eq. (31) as

$$\nabla^2\delta\phi_p = \frac{4\pi q^2 n(r,z)}{T}(\delta\phi_p(r,z) + \delta\phi_{ext}(r,z) - \int dz' M(r,z,z')\left[\delta\phi_p(r,z') + \delta\phi_{ext}(r,z')\right]), \tag{A1}$$

where the kernel function $M(r,z,z')$ is defined as

$$M(r,z,z') = \frac{4m}{\sqrt{2\pi T}}\int_{v_{z\min}(r,z,z')}^{\infty} dv_z \times \frac{e^{-mv_z^2/2T}}{\tau(r, mv_z^2/2 + \phi(r,z))\sqrt{mv_z^2 + 2\phi(r,z) - 2\phi(r,z')}}. \tag{A2}$$

The minimum velocity in the integration, $v_{z\min}$, is the minimum speed at point z required for a particle orbit to reach point z'. This speed depends on whether z and z' are located on the same side or on the opposite sides of the maximum of the squeeze potential at $z = z_s(r)$, given by $\phi_s(r) \equiv \phi(r,z_s)$. If both z and z' are on the same side of the maximum [i.e., $\mathrm{sign}(z - z_s) = \mathrm{sign}(z' - z_s)$], then $v_{z\min} = \sqrt{(2/m)\mathrm{Max}(0, \phi(r,z') - \phi(r,z))}$. But, if z and z' are on the opposite sides of the maximum, then

$$v_{z\min} = \mathrm{Max}(\sqrt{(2/m)\mathrm{Max}(0, \phi(r,z') - \phi(r,z))}, \sqrt{(2/m)\mathrm{Max}(0, \phi_s(r) - \phi(r,z))}). \tag{A3}$$

When evaluating Eq. (A1) on the grid, we approximate

$$\int dz' M(r,z_i,z')f(z') \simeq \Delta z \sum_j M(r,z_i,z_j)f(z_j) \tag{A4}$$

for any function $f(z)$, where Δz is the z grid spacing. However, the form for the kernel function must be modified for the case $z_i = z_j$. Here, the integrand in Eq. (A2) is logarithmically divergent as $v_z \to 0$, and at this grid point, we must regularize by replacing $M(r,z_i,z_i)$ with $\bar{M}(r,z_i) \equiv \Delta z^{-1}\int_{z_i-\Delta z/2}^{z_i+\Delta z/2} dz' M(r,z_i,z')$. Since z' is close to z_i, we can Taylor expand the integrand in Eq. (A2), writing

$$\bar{M}(r,z_i) = \Delta z^{-1}\int_{z_i-\Delta z/2}^{z_i+\Delta z/2} dz' \frac{4m}{\sqrt{2\pi T}}\int_{\sqrt{\mathrm{Max}(0,a)}}^{\infty} dv_z \times \frac{e^{-mv_z^2/2T}}{\tau(r, mv_z^2/2 + \phi(r,z_i))\sqrt{mv_z^2 + 2(z'-z_i)E(r,z_i)}}, \tag{A5}$$

where $E(r,z) = -\partial\phi/\partial z$ and $a = (2/m)(z_i - z')E$. We will separate out the logarithmic divergence by breaking the velocity integral into $\int_{\sqrt{\mathrm{Max}(0,a)}}^{\epsilon} dv_z + \int_{\epsilon}^{\infty} dv_z$, where

$\epsilon = \sqrt{|E\Delta z/m|}$ is a small velocity. In the first velocity integral, the Maxwellian and bounce time can be evaluated at $v_z = 0$ and the velocity integral can then be performed, yielding

$$\bar{M}(r,z_i) = \frac{4}{\Delta z\sqrt{2\pi T/m}\tau(r,\phi(r,z_i))} \times \int_{z_i-\Delta z/2}^{z_i+\Delta z/2} dz' \left(\log\left[\epsilon + \sqrt{\epsilon^2 - a}\right] - \log|a|/2\right) + \frac{4m}{\Delta z\sqrt{2\pi T}} \int_{z_i-\Delta z/2}^{z_i+\Delta z/2} dz' \int_{\epsilon}^{\infty} dv_z \times \frac{e^{-mv_z^2/2T}}{\tau(r, mv_z^2/2 + \phi(r,z_i))\sqrt{mv_z^2 + 2(z'-z_i)E(r,z_i)}}. \tag{A6}$$

In both the first and second integrals, the z' integration can now be performed analytically, yielding

$$\bar{M}(r,z_i) = \frac{4}{\sqrt{2\pi T/m}\tau(r,\phi(r,z_i))}\left(\frac{1}{2}\log\left[\sqrt{2}+1/\sqrt{2}\right] + \frac{1}{\sqrt{2}}\right) + \frac{4}{\epsilon^2\sqrt{2\pi T/m}} \int_{\epsilon}^{\infty} dv_z \frac{e^{-mv_z^2/2T}\left(\sqrt{v_z^2+\epsilon^2} - \sqrt{v_z^2-\epsilon^2}\right)}{\tau(r, mv_z^2/2 + \phi(r,z_i))}. \tag{A7}$$

For a given plasma equilibrium density $n(r, z)$ and self-consistent equilibrium potential $\phi(r, z)$, we solve Eq. (A1) on a grid in r and z by first evaluating $\bar{M}(r, z, z')$ on the grid using Eq. (A2) [or Eq. (A6) when $z = z'$]. This requires determining the bounce period $\tau(r, E_z)$ in the given potential $\phi(r, z)$ using Eq. (9), and then performing the required velocity integrations in Eq. (A2) [or Eq. (A6)] numerically. Note that the bounce period has a different functional form on the left and right sides of the squeeze (i.e., $z < z_s$ and $z > z_s$, respectively) and is singular at the separatrix energy where $E_z = \phi_s(r)$. Evaluations of $\bar{M}$ at each grid point are required only for points within the plasma; in the vacuum region between the plasma and the wall at $r = r_w$, we can set $\bar{M} = 0$. For a thin plasma compared with the wall radius, this fact greatly speeds up the computation. We then formulate Eq. (A1) as a linear matrix equation $K_{i,j}\delta\phi_{pj} = \delta\rho_j$, where j counts over the $r - z$ grid and the inhomogeneous terms $\delta\rho_j$ are those terms in Eq. (A1) involving $\delta\phi_{ext}$, which is a given function determined by the voltages on the cylindrical electrodes. The radial and axial derivatives are finite-differenced using standard second-order centered differences. We solve this matrix problem numerically using the SLATEC subroutine SGEFS.

APPENDIX B: NONADIABATIC EFFECTS FOR AN OSCILLATORY EXTERNAL POTENTIAL

Here, we consider collisionless non-adiabatic corrections to the velocity distribution function caused by slow time oscillation of the external potential $\delta\phi_{ext}(z)\cos(\omega t)$ (we suppress radial dependence for notational convenience). These non-adiabatic corrections are small when the oscillation frequency ω is small compared with the bounce frequency ω_b, but can still be observed in the experiments. These corrections can be determined by solving the Vlasov equation using action-angle variables (I, ψ), where $I = J/(2\pi)$. In these variables, the perturbed distribution function then satisfies the linearized Vlasov equation

$$\frac{\partial \delta f}{\partial t} + \omega_b(I)\frac{\partial \delta f}{\partial \psi} - \frac{\partial \delta\phi}{\partial \psi}\frac{\partial f}{\partial I} = 0, \tag{B1}$$

where the bounce frequency $\omega_b = 2\pi/\tau$. For f a Maxwellian, $\partial f/\partial I = -(f/T)\partial E_z/\partial I = -f\omega_b/T$. The perturbed distribution function δf and the perturbed potential $\delta\phi$ are assumed to be periodic in time with the same frequency ω as the forcing

$$\delta\phi(z,t) = \mathrm{Re}\delta\Phi(z)e^{-i\omega t},$$
$$\delta f(z, v_z, t) = \mathrm{Re}\delta F(z, v_z)e^{-i\omega t},$$

where $\delta\Phi$ and δF are complex amplitudes. Noting that ψ is a periodic variable, so that δF and $\delta\Phi$ are both periodic in ψ, one may Fourier-expand these functions in ψ

$$\delta\Phi = \sum_{n=-\infty}^{\infty} \delta\phi_n(I)e^{in\psi}, \tag{B2}$$

$$\delta F = \sum_{n=-\infty}^{\infty} \delta f_n(I)e^{in\psi}. \tag{B3}$$

Then, Eq. (B1) becomes

$$-i\omega\delta f_n + in\omega_b\delta f_n + in\omega_b f\delta\phi_n/T = 0, \tag{B4}$$

with solution

$$\delta f_n = -f\frac{\delta\phi_n}{T}\frac{n\omega_b}{n\omega_b - \omega}. \tag{B5}$$

Note that this equation implies that $\delta f_0 = 0$. This $n = 0$ Fourier component is zero because this is the bounce-averaged portion of the perturbed distribution function [the ψ-independent part; see Eq. (B3)]. For this term, the linearized Vlasov equation merely phase-mixes the distribution function along unperturbed orbits in phase space, which by conservation of particle number and phase-space area implies that the bounce-averaged distribution function is unaffected by potential perturbations. This was also seen by bounce-averaging the adiabatic form of δf [see Eq. (18)], but here, we see that the result also applies to the fully nonadiabatic distribution.

For $n \neq 0$, Eq. (B5) can be rewritten in a useful way by subtracting and adding ω in the numerator, yielding

$$\delta f_n = -f\frac{\delta\phi_n}{T}\left(1 + \frac{\omega}{n\omega_b - \omega}\right). \tag{B6}$$

Substitution into Eq. (B3) and application of Eq. (B2) in order to re-sum the Fourier series for $\delta\phi$ then yield

$$\delta F = -\frac{f}{T}\left(\delta\Phi - \delta\phi_0 + \sum_{n=-\infty,n\neq 0}^{\infty} \delta\phi_n e^{in\psi}\frac{\omega}{n\omega_b - \omega}\right). \quad \text{(B7)}$$

Noting that $\mathrm{Re}\delta\phi_0 e^{-i\omega t} = \langle\delta\phi\rangle$, the first two terms in the parentheses are identical to the terms appearing in the adiabatic response as given by Eq. (17). Thus, the remaining term involving a sum over bounce harmonics yields the nonadiabatic contribution to the perturbed distribution function. This term vanishes as ω approaches zero, as one might expect.

The full nonadiabatic form for δF keeps all physics associated with linear Landau damping through the appearance of the resonant denominator in Eq. (B7). However, for low-frequencies, one can Taylor-expand this denominator, which effectively neglects any Landau damping and associated filamentation of δF, and results in the slightly simpler expression

$$\delta F \approx -\frac{f}{T}\left(\delta\Phi - \delta\phi_0 + \frac{\omega}{\omega_b}\sum_{n=-\infty,n\neq 0}^{\infty}\frac{\delta\phi_n}{n}e^{in\psi}\right). \quad \text{(B8)}$$

This expression can be put back into (z, v_z) coordinates by means of the following argument. The last term in the parenthesis (the nonadiabatic term) can be written as

$$\frac{\omega}{\omega_b}\sum_{n=-\infty,n\neq 0}^{\infty}\frac{\delta\phi_n}{n}e^{in\psi} = \frac{i\omega}{\omega_b}\sum_{n=-\infty,n\neq 0}^{\infty}\delta\phi_n\left(\int_0^{\psi} e^{in\psi}d\psi + \frac{1}{in}\right). \quad \text{(B9)}$$

However, if ψ is defined using the condition that $\psi = 0$ at the left turning point $z = z_1$ (so that $\psi = \pi$ at $z = z_2$), then it follows that $\delta\phi_n$ is even in n, so the term $\delta\phi_n/in$ can be dropped because the sum is antisymmetric in n. This is because according to Eq. (B2),

$$\begin{aligned}\delta\phi_n &= \int_0^{2\pi}\frac{d\psi}{2\pi}\delta\Phi(z(I,\psi))e^{-in\psi}\\ &= \frac{2}{\tau}\int_{z_1}^{z_2}\frac{dz}{V_z(E_z,z)}\delta\Phi(z)\cos\left(n\psi(I,z)\right),\end{aligned} \quad \text{(B10)}$$

where the second form has converted the integral over ψ to one over z using the action-angle relation $\partial z/\partial\psi|_I = v_z/\omega_b$, after breaking the integral over ψ into one running from 0 to π, for which z runs from z_1 to z_2 with $v_z > 0$, and one running from π to 2π, for which z runs from z_2 to z_1 with $v_z < 0$. This equation shows explicitly that $\delta\phi_n$ is even in n, so one can drop the odd $\delta\phi_n/in$ term in the sum in Eq. (B9) and re-sum the Fourier series using Eq. (B2), to obtain the lowest-order nonadiabatic contribution $\delta F^{(na)}$ to δF

$$\begin{aligned}\delta F^{(na)} &\equiv -\frac{\omega f}{\omega_b T}\sum_{n=-\infty,n\neq 0}^{\infty}\frac{\delta\phi_n}{n}e^{in\psi - i\omega t}\\ &= -\frac{i\omega f}{\omega_b T}\int_0^{\psi} d\psi(\delta\Phi - \langle\delta\Phi\rangle).\end{aligned} \quad \text{(B11)}$$

Again using $\partial z/\partial\psi|_I = v_z/\omega_b$ and assuming that $v_z > 0$ so that $0 < \psi < \pi$, the integral over ψ transforms to

$$\delta F^{(na)} = -\frac{i\omega f}{T}\int_{z_1}^{z}\frac{dz'}{V_z(E_z,z')}(\delta\Phi(z') - \langle\delta\Phi\rangle(E_z)), \quad v_z > 0. \quad \text{(B12)}$$

For $v_z < 0$, $\psi > \pi$, so we break the ψ integral in Eq. (B11) into a portion that runs from $\psi = 0$ to $\psi = \pi$ (for which z' runs from z_1 to z_2), and an integral from π to ψ (for which $v_z < 0$ and z' runs from z_2 back to z)

$$\begin{aligned}\delta F^{(na)} = &-\frac{i\omega f}{T}\int_{z_1}^{z_2}\frac{dz'}{V_z(E_z,z')}(\delta\Phi(z') - \langle\delta\Phi\rangle(E_z))\\ &+\frac{i\omega f}{T}\int_{z_2}^{z}\frac{dz'}{V_z(E_z,z')}(\delta\Phi(z') - \langle\delta\Phi\rangle(E_z)), \quad v_z < 0.\end{aligned} \quad \text{(B13)}$$

However, the first integral vanishes due to the definition of the bounce average, see Eq. (8). We may therefore change the sign of this term without changing the result, leading to

$$\delta F^{(na)} = \frac{i\omega f}{T}\int_{z_1}^{z}\frac{dz'}{V_z(E_z,z')}(\delta\Phi(z') - \langle\delta\Phi\rangle(E_z)), \quad v_z < 0. \quad \text{(B14)}$$

Since E_z is even in v_z, Eqs. (B12) and (B14) show that $\delta F^{(na)}$ is odd in v_z; as opposed to the adiabatic distribution given by Eq. (17), which is even in v_z. This provides a useful way to distinguish the adiabatic and nonadiabatic contributions to the distribution function in the experiments. Also, this implies that the nonadiabatic distribution makes no contribution to the perturbed density or potential; but it does produce a perturbed fluid velocity $\delta U_z(z,t)$

$$\begin{aligned}n\delta U_z &= \int dv_z v_z \mathrm{Re}\delta F^{(na)}e^{-i\omega t}\\ &= -\int v_z dv_z \mathrm{Sign}(v_z)\int_{z_1}^{z}\frac{dz'}{V_z(E_z,z')}\frac{\partial}{\partial t}\delta f,\end{aligned} \quad \text{(B15)}$$

where we have substituted for δF^{na} using Eqs. (B12) and (B14), $\delta f(E_z, z', t)$ is the adiabatic distribution given by Eq. (17), and we have used $\mathrm{Re}i\omega\delta F e^{-i\omega t} = -\partial f/\partial t$. Reordering the integration yields

$$n\delta U_z = -\frac{\partial}{\partial t}\int_{-\infty}^{z} dz'\int dv_z\delta f = -\frac{\partial}{\partial t}\int_{-\infty}^{z} dz'\delta n(z',t), \quad \text{(B16)}$$

where δn is the adiabatic density change. This implies that the particle flux from the nonadiabatic fluid velocity δU_z produces the adiabatic density change δn, as expected from the linearized continuity equation

$$\frac{\partial}{\partial z}(n\delta U_z) = -\frac{\partial}{\partial t}\delta n. \tag{B17}$$

The nonadiabatic distribution can be simplified further for the case of particles undergoing specular reflections in a central squeeze potential and slowly moving end walls, and neglecting self-consistent effects [i.e., the model discussed previously in relation to Eqs. (19)–(27)]. We will simplify further by assuming that $\delta L_1 = -\delta L_2 \equiv \delta L$, i.e., both ends move in the same direction, with the same amplitude, as in Fig. 1. For this case, we found that the end potentials satisfy $\delta\phi = -\delta L(t)\partial\phi/\partial z$; see the discussion preceding Eq. (21). Using this in Eqs. (B12) and (B14) and assuming passing particles, for which the system symmetry implies $\langle\delta\phi\rangle = 0$, the same operations as were used in deriving Eq. (21) yield

$$\delta F^{(na)} = -\frac{mv_z f}{T} i\omega\delta L, \quad mv_z^2 > 2\phi_s. \tag{B18}$$

This is the expected result for the passing particles in the absence of collective effects: $\mathrm{Re}\delta F^{na} e^{-i\omega t}$ is the first-order correction to a shifted Maxwellian distribution of the form $\exp\left[-m(v_z - \delta\dot{L})^2/(2T)\right]/\sqrt{2\pi T/m}$. For passing particles, the slowly moving walls simply cause the plasma to move along with the walls.

When collective effects are included in this specular-reflection model, however, there is an extra term in the perturbed potential caused by density changes, and given by the solution to Eq. (27). When this potential is added to Eqs. (B12) and (B14) and the z-integral is performed, one obtains

$$\delta F^{(na)} = -\frac{mv_z f}{T} i\omega\delta L - \frac{f}{Tv_z} i\omega \begin{Bmatrix} \delta\phi_{p,1} z, & z < L_1 \\ -\delta\phi_{p,2}(L - z), & z > L_1 \end{Bmatrix}, \quad mv_z^2 > 2\phi_s. \tag{B19}$$

This extra term in $\delta F^{(na)}$ is caused by passing particles sloshing from one end of the plasma to the other as they Debye-shield the potential produced by the trapped particles. Note that since $L_1\delta\phi_{p,1} + L_2\delta\phi_{p,2} = 0$ (see Eq. (26) for the case $\delta L_1 + \delta L_2 = 0$), the distribution is continuous across the squeeze barrier at $z = L_1$.

On the other hand, for trapped particles, this extra self-consistent potential does not affect δf because, for these particles, $\delta\phi_{p,j} = \langle\delta\phi_{p,j}\rangle$. However, the end potential due to the moving walls is still $\delta\phi = -\delta L\partial\phi/\partial z$, but now $\langle\delta\phi\rangle$ is given by Eq. (21) (for particles to the left of the squeeze, with a change in sign for particles to the right). Using these results in Eqs. (12) and (B14), and noting that $z_1 = 0$ for trapped particles on the left and $z_1 = L_1$ for trapped particles on the right yield, after some work,

$$\delta F^{(na)} = -\frac{mv_z}{T} f(L_1 - z) i\omega \begin{Bmatrix} \delta L/L_1, & z < L_1 \\ -\delta L/L_2, & z > L_1 \end{Bmatrix}, \quad mv_z^2 < 2\phi_s. \tag{B20}$$

At the plasma ends ($z = 0$ and $z = L$), Eqs. (B19) and (B20) reduce to $\delta F^{(na)} = -(mv_z f/T) i\omega\delta L$, which implies that the perturbed fluid velocity at the ends is $\delta U_z = \partial\delta L/\partial t$. Thus, as expected, the fluid velocity matches that of the moving ends.

[1] A. A. Galeev, R. Z. Sagdeev, H. P. Furth, and M. N. Rosenbluth, Phys. Rev. Lett. **22**, 511 (1969).
[2] M. N. Rosenbluth, D. W. Ross, and D. P. Kostamorov, Nucl. Fusion **12**, 3 (1972).
[3] H. Mynick, Phys. Plasmas **13**, 058102 (2006).
[4] D. H. E. Dubin and Y. A. Tsidulko, Phys. Plasmas **18**, 062114 (2011).
[5] D. H. E. Dubin, C. F. Driscoll, and Y. A. Tsidulko, Phys. Rev. Lett. **105**, 185003 (2010).
[6] B. P. Cluggish, J. R. Danielson, and C. F. Driscoll, Phys. Rev. Lett. **81**, 353 (1998).
[7] B. R. Beck, J. Fajans, and J. H. Malmberg, Phys. Plasmas **3**, 1250 (1996).
[8] A. Lenard and I. B. Bernstein, Phys. Rev. **112**, 1456 (1958).
[9] M. Affolter, F. Anderegg, D. H. E. Dubin, and C. F. Driscoll, Phys. Rev. Lett. **117**, 155001 (2016).
[10] S. Chapman and T. Cowling, *The Mathematical Theory of Nonuniform Gases* (Cambridge University Press, 1960).
[11] F. A. Angona, "The absorption of sound in gas mixtures," Technical Report No. V, Project NR014-302 (Office of Naval Research, 1953).
[12] F. Anderegg, M. Affolter, D. Dubin, and C. F. Driscoll, "Nonresonant particle heating due to collisional separatrix crossing," (unpublished).
[13] A. A. Kabantsev, Y. A. Tsidulko, and C. F. Driscoll, Phys. Rev. Lett. **112**, 055003 (2014).
[14] A. A. Kabantsev, T. M. O'Neil, Y. A. Tsidulko, and C. F. Driscoll, Phys. Rev. Lett. **101**, 065002 (2008).
[15] T. J. Hilsabeck, A. A. Kabantsev, C. F. Driscoll, and T. M. O'Neil, Phys. Rev. Lett. **90**, 245002 (2003).
[16] A. A. Kabantsev, C. F. Driscoll, D. H. E. Dubin, and Y. A. Tsidulko, J. Plasma Phys. **81**, 305810105 (2014).
[17] D. H. E. Dubin, A. A. Kabantsev, and C. F. Driscoll, Phys. Plasmas **19**, 056102 (2012).
[18] A. A. Kabantsev, D. H. E. Dubin, C. F. Driscoll, and Y. A. Tsidulko, Phys. Rev. Lett. **105**, 205001 (2010).
[19] D. H. E. Dubin, Phys. Plasmas **15**, 072112 (2008).
[20] S. A. Prasad and T. M. O'Neil, Phys. Fluids **22**, 278 (1979).
[21] A. Ashourvan and D. H. E. Dubin, J. Plasma Phys. **81**, 305810202 (2015).